

## Anisotropic stress relief mechanism in epitaxial $\text{La}_{0.67}\text{Sr}_{0.33}\text{MnO}_3$ films

Arturas Vailionis,<sup>1</sup> Hans Boschker,<sup>2</sup> Evert Houwman,<sup>2</sup> Gertjan Koster,<sup>2,a)</sup> Guus Rijnders,<sup>2</sup> and Dave H. A. Blank<sup>2</sup>

<sup>1</sup>Geballe Laboratory for Advanced Materials, Stanford University, Stanford, California 94305, USA

<sup>2</sup>MESA<sup>+</sup> Institute for Nanotechnology, University of Twente, 7500 AE Enschede, The Netherlands

(Received 23 July 2009; accepted 23 September 2009; published online 14 October 2009)

We report an anisotropic misfit stress relief mechanism in thin  $\text{La}_{0.67}\text{Sr}_{0.33}\text{MnO}_3$  (LSMO) films coherently grown on  $\text{NdGaO}_3(110)$  substrates. These results are uniquely related to the orthorhombicity of the LSMO. The x-ray diffraction measurements and quantitative simulations demonstrate that biaxial mismatch stress is relieved differently along in-plane directions perpendicular to each other: in the  $[1\bar{1}0]$  direction stress is accommodated by decrease of the  $\gamma$  angle of the orthorhombic LSMO unit cell, while in the  $[001]$  direction stress is partially relieved by periodic lattice modulations. © 2009 American Institute of Physics. [doi:10.1063/1.3249583]

The discovery of colossal magnetoresistance, the variation of electrical resistance with magnetic field, in doped  $\text{La}_{1-x}\text{A}_x\text{MnO}_3$  (A is an alkaline earth element=Ba, Sr, Ca) thin films has initiated a substantial interest in La-based manganites due to a possible practical application of their magnetoresistive properties in magnetic data storage.<sup>1,2</sup> Extensive theoretical studies and experimental investigations utilizing  $\text{La}_{1-x}\text{A}_x\text{MnO}_3$  perovskites in bulk form revealed a strong coupling between lattice distortions and magnetism, which substantially modify magnetic properties such as magnetoresistance and Curie temperature.<sup>3,4</sup> The local lattice distortions in bulk manganites (changes in Mn–O bond lengths and/or Mn–O–Mn bond angles) are usually induced by hydrostatic or chemical pressure and can be quantified using such techniques as extended x-ray absorption fine structure and x-ray or neutron diffraction.<sup>5–7</sup> For thin epitaxial  $\text{La}_{1-x}\text{Sr}_x\text{MnO}_3$  films the substrate-induced biaxial stress has been known to be an effective tool to modify the electron-lattice coupling and the magnetic properties.<sup>8–12</sup> Recent magnetic anisotropy measurements of epitaxial  $\text{La}_{0.67}\text{Sr}_{0.33}\text{MnO}_3$  (LSMO) films grown on  $\text{NdGaO}_3(110)$  [NGO(110)] substrates link the observed uniaxial magnetic anisotropy to a dissimilar in-plane lattice mismatch between the layer and the substrate along perpendicular directions of the NGO(110) substrate.<sup>13</sup>

In this letter we investigate the microstructure of the LSMO layer grown on NGO(110), using high-resolution x-ray diffraction (XRD). We demonstrate that the LSMO layers grown on NGO(110) substrate possess a slightly distorted orthorhombic (monoclinic) structure with  $[110]$  out-of-plane growth direction. Moreover, XRD measurements and quantitative XRD simulations show a distinctive anisotropic stress relief mechanism along the perpendicular  $[1\bar{1}0]$  and  $[001]$  in-plane directions of the orthorhombic LSMO unit cell. In the  $[1\bar{1}0]$  direction the stress is effectively accommodated by a decrease of the  $\gamma$ -angle, while stress in the  $[001]$  direction is partially reduced by periodic out-of-plane lattice modulations with an amplitude of 0.18 Å and in-plane periodicity of  $\Lambda=23$  nm. The high-temperature XRD measurements reveal that at higher temperatures the observed lattice

modulations disappear due to an orthorhombic-to-tetragonal phase transition.

The epitaxial LSMO films were grown on NGO(110) substrates by pulsed laser deposition at 800 °C from a stoichiometric target in an oxygen background pressure of 0.16–0.27 mbar. A KrF excimer laser ( $\lambda=248$  nm) was used with a fluence of 2 J/cm<sup>2</sup> and a pulse repetition rate of 5 Hz. The target to substrate distance was fixed at 5 cm. After deposition, the films were cooled down to room temperature at a rate of 10 °C/min in a 1 bar pure oxygen atmosphere. Atomic force microscopy measurements showed smooth surfaces with unit cell high steps. XRD measurements were performed using a PANalytical X'Pert materials research diffractometer in high- and medium-resolution modes at the Stanford Nanocharacterization Laboratory, Stanford University. High temperature measurements were performed using an Anton–Paar hot stage.

The XRD results demonstrate that epitaxially grown  $\text{La}_{0.67}\text{Sr}_{0.33}\text{MnO}_3$  films are twin-free and possess a distorted orthorhombic (monoclinic) unit cell with (110) out-of-plane orientation and  $(1\bar{1}0)$  and (001) in-plane orientations. Figure 1 shows reciprocal lattice maps of the LSMO and NGO (260), (444), (620), and  $(44\bar{4})$  reflections. As can be seen from the figure, the LSMO layer grown on NGO(110) substrate exhibits an orthorhombic unit cell, symbolized by the difference in LSMO (260) and (620) atomic plane spacings, which represent a dissimilarity between the  $a$  and  $b$  lattice parameters. The refined lattice parameters of 40 nm thick LSMO film are as follows:  $a=5.477$  Å,  $b=5.513$  Å,  $c=7.707$  Å,  $\alpha=\beta=90.0^\circ$ , and  $\gamma=89.32^\circ$ . Figure 2(a) shows XRD in-plane scans around LSMO( $hk0$ ) Bragg peak positions with  $h=k=1, 2, 3$ , and 4. It is important to note, that the x-ray beam direction in this case was aligned in the LSMO $[001]$  direction. Besides the Bragg peaks, satellite peaks which originate from periodic lattice modulations in the  $[001]$  direction are clearly visible. The calculated period of the long range modulation is  $\Lambda=23$  nm, roughly equal to 30 LSMO unit cells with  $c=7.707$  Å. XRD measurements reveal that the lattice modulations are present only in the  $[001]$  in-plane direction and are absent in the  $[1\bar{1}0]$  direction. Figure 2(b) shows reciprocal lattice maps around symmetric LSMO(220) Bragg peak with x-ray beam aligned parallel to

<sup>a)</sup>Electronic mail: g.koster@utwente.nl.

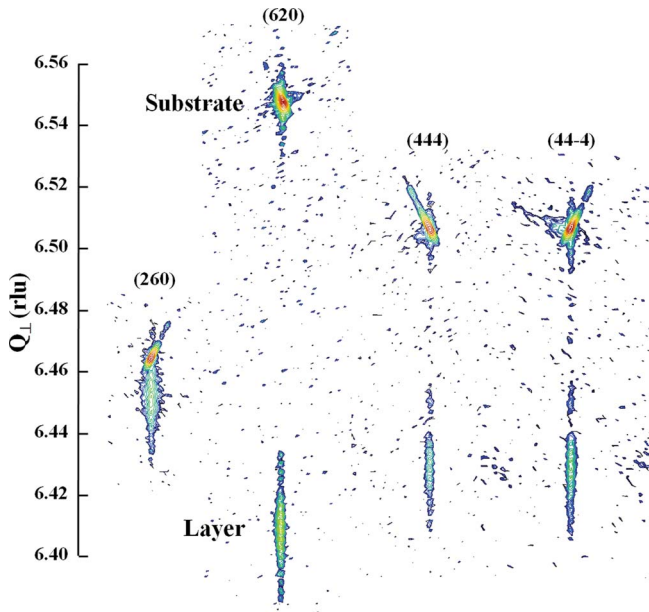


FIG. 1. (Color online) Room temperature reciprocal space maps of the LSMO and NGO (260), (444), (620), and (44 $\bar{4}$ ) Bragg reflections. Here we used  $Q = 4\pi \sin \theta / \lambda$  where  $\theta$  is the Bragg angle and  $\lambda = 1.540\,598$  Å.

the [001] axis and parallel to the  $[1\bar{1}0]$  axis. The satellites are clearly visible only in reciprocal space maps (RLMs) taken in the [001] direction. They are absent in the  $[1\bar{1}0]$  direction, indicating the highly anisotropic nature of the lattice modulations.

The observed lattice modulations can be quantitatively described using a kinematical XRD model. We assume that the unit cells have displacements in the  $[110]$  direction with amplitude  $A_L$ , which are periodic in the [001] direction, with

periodicity  $\Lambda$ . In order to account for the satellite peak broadening, we assume that modulation period deviates from a mean value  $\Lambda = 23$  nm according to a Gaussian distribution with a standard deviation  $\delta\Lambda$ . The simulation results, together with the experimental data are shown in Fig. 2(a). As can be seen, the calculations reproduce all features of the four ( $hk0$ ) XRD spectra: main Bragg peak, satellite peak positions, intensities, and widths using a single set of parameters,  $\Lambda = 23$  nm,  $A_L = 0.18$  Å, and  $\delta\Lambda = 5$  nm. The simulations were also performed assuming displacements of the unit cells in the in-plane  $[1\bar{1}0]$  direction. The calculations did not produce satisfactory results, indicating that unit cell displacements occur only in the out-of-plane direction. This is consistent with coherent layer growth on a single crystal substrate.

It is known that such lattice modulations help to relieve stress originating from the mismatch strain between the LSMO layer and the underlying substrate, as found by Vigliante *et al.* and Gebhardt *et al.*<sup>14,15</sup> These authors observed biaxial LSMO lattice modulations aligned along perpendicular in-plane  $[100]$  and  $[010]$  directions of a cubic SrTiO<sub>3</sub>(001) substrate. The observed modulation anisotropy in our samples can only be described by taking into consideration the orthorhombic LSMO unit cell with (110) out-of-plane orientation and a mismatch between LSMO and NGO unit cells in the in-plane  $[1\bar{1}0]$  and [001] directions of 0.79% and 1.02%, respectively.<sup>16</sup> In the  $[1\bar{1}0]$  direction the orthorhombic LSMO unit cell accommodates stress by utilizing the “softness” of the  $\gamma$ -angle, which for the strained layer is reduced to 89.32°. Such stress accommodation has also been observed in epitaxial SrRuO<sub>3</sub>(110) films.<sup>17</sup> It is important to note, that the stress in the (orthorhombic)  $a$  and  $b$  lattice directions is almost entirely relieved by the  $\gamma$ -angle reduction, leaving only small compressive strain components of  $-0.2\%$ . The in-plane direction perpendicular to  $[1\bar{1}0]$  does not have such an additional degree of freedom. The observed lattice modulation with an amplitude of 0.18 Å is not able to substantially relieve the stress imposed by the substrate. Therefore, the resulting compressive strain in the  $c$ -axis direction remains rather large  $-1.02\%$ , as compared to the strain values in the  $a$  and  $b$  directions.

Interestingly, the lattice modulations tend to disappear at higher temperatures. Figure 3 shows RLMs of the LSMO(220) peak in the [001] direction at 25, 50, 400, and 500 °C. The satellites are visible at 25, 50, and 400 °C and are absent at 500 °C. The RLM at 25 °C was taken after the sample was cooled down demonstrating that the lattice modulations are reversible with thermal cycling. Figure 3 also shows the dependence of the LSMO  $a$  and  $b$  lattice parameters as function of temperature. The presented data points are taken during heating and are completely identical during cooling. The difference between the  $a$  and  $b$  lattice constants decreases as the temperature is increased. The high-temperature XRD data indicate that, as the satellite peaks disappear, the LSMO unit cell transforms from orthorhombic into a more symmetric, tetragonal form. As can be seen from Fig. 3, the orthorhombicity factor ( $a/b$  ratio) of LSMO unit cell does not follow the trend of the NGO lattice and the point of  $a=b$  is reached at temperatures of  $\sim 850$  K. Such a structural phase transition is clearly related to rotations of the MnO<sub>6</sub> octahedra.<sup>18</sup> The main difference between

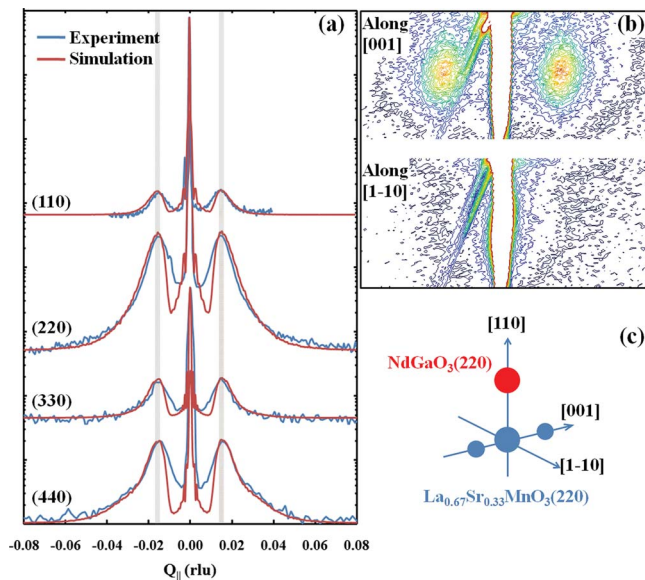


FIG. 2. (Color online) Lattice modulations observed by XRD: (a) in-plane scans around LSMO( $hk0$ ) reflections with  $h=k=1,2,3,4$ . The gray vertical lines are guides to the eye and show that satellite peaks originate from periodic displacements of the unit cells and not from out-of-plane twinning, (b) RLM around LSMO(220) reflection with incident beam aligned in the [001] (top) and  $[1\bar{1}0]$  (bottom) directions, (c) schematic picture of a reciprocal space showing NGO(220) peak (red) and LSMO(220) peak and satellites (blue).

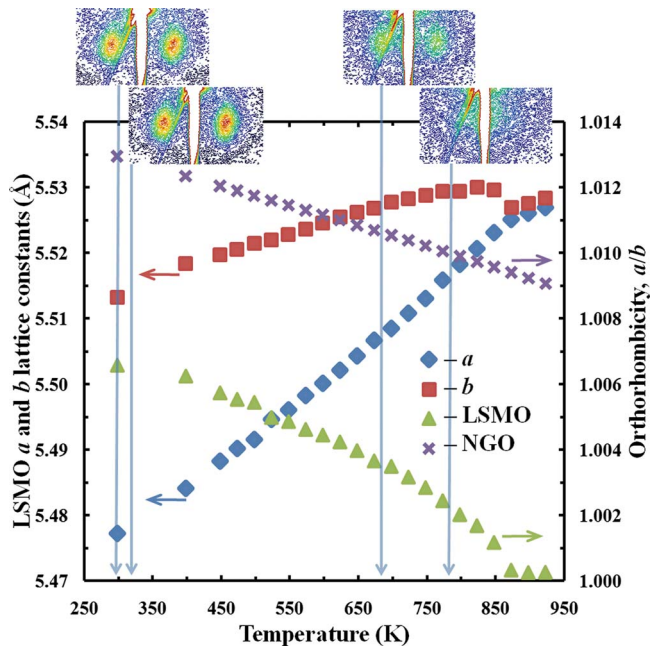


FIG. 3. (Color online) LSMO  $a$  and  $b$  lattice constants and orthorhombicity factor of LSMO thin film and NGO substrate as a function of temperature indicating orthorhombic to tetragonal structural phase transition at high temperatures. Reciprocal lattice maps around LSMO(220) Bragg peaks indicate that the satellite peaks disappear at  $\sim 500$  °C but reappear on cool down.

the orthorhombic and tetragonal unit cell is the absence of octahedra rotations in the  $[001]$  direction. As the LSMO unit cell transforms from orthorhombic to tetragonal, the long range lattice modulations disappear indicating a strong link between  $\text{MnO}_6$  octahedra rotations and stress accommodation by lattice modulations.

In summary, we report an anisotropic stress relief mechanism in epitaxial  $\text{La}_{0.67}\text{Sr}_{0.33}\text{MnO}_3$  thin films grown on  $\text{NdGaO}_3(110)$  single crystal substrates. Thin LSMO films have an orthorhombic unit cell with  $[110]$  out-of-plane growth direction. In the  $[1\bar{1}0]$  in-plane direction the compressive stress of the crystallographic  $a$  and  $b$  axes of the unit cell is effectively relieved by a reduction of the  $\gamma$ -angle. In the  $[001]$  direction a relatively large compressive stress is only marginally accommodated by periodic lattice modulations. The lattice modulations disappear as LSMO transforms from the low symmetry orthorhombic phase into the higher

symmetry tetragonal phase. Such a correlation strongly links  $\text{MnO}_6$  octahedra rotations to the lattice modulations in the  $[001]$  direction. Finally, we suspect that this anisotropic stress relief mechanism is operative in other orthorhombic perovskite thin films as well.

This research was financially supported by the Dutch Science Foundation and by NanoNed, a nanotechnology program of the Dutch Ministry of Economic Affairs.

- <sup>1</sup>R. von Helmolt, J. Wecker, B. Holzapfel, L. Schultz, and K. Samwer, *Phys. Rev. Lett.* **71**, 2331 (1993).
- <sup>2</sup>S. Jin, T. H. Tiefel, M. McCormack, R. A. Fastnacht, R. Ramesh, and L. H. Chen, *Science* **264**, 413 (1994).
- <sup>3</sup>Y. Moritomo, A. Asamitsu, and Y. Tokura, *Phys. Rev. B* **51**, 16491 (1995).
- <sup>4</sup>H. Y. Hwang, T. T. M. Palstra, S.-W. Cheong, and B. Batlogg, *Phys. Rev. B* **52**, 15046 (1995).
- <sup>5</sup>E. O. Wollan and W. C. Koehler, *Phys. Rev.* **100**, 545 (1955).
- <sup>6</sup>C. H. Booth, F. Bridges, G. H. Kwei, J. M. Lawrence, A. L. Cornelius, and J. J. Neumeier, *Phys. Rev. Lett.* **80**, 853 (1998).
- <sup>7</sup>H. Y. Hwang, S.-W. Cheong, P. G. Radaelli, M. Marezio, and B. Batlogg, *Phys. Rev. Lett.* **75**, 914 (1995).
- <sup>8</sup>Y. Suzuki, H. Y. Hwang, S.-W. Cheong, and R. B. van Dover, *Appl. Phys. Lett.* **71**, 140 (1997); Y. Suzuki, H. Y. Hwang, S.-W. Cheong, T. Siegrist, R. B. van Dover, A. Asamitsu, and Y. Tokura, *J. Appl. Phys.* **83**, 7064 (1998).
- <sup>9</sup>C. Kwon, M. C. Robson, K.-C. Kim, J. Y. Gu, S. E. Lofland, S. M. Bhagat, Z. Trajanovic, M. Rajeswari, T. Venkatesan, A. R. Kratz, R. D. Gomez, and R. Ramesh, *J. Magn. Magn. Mater.* **172**, 229 (1997).
- <sup>10</sup>M. Mathews, F. M. Postma, J. Cock Lodder, R. Jansen, G. Rijnders, and D. H. A. Blank, *Appl. Phys. Lett.* **87**, 242507 (2005).
- <sup>11</sup>F. Tsui, M. C. Smoak, T. K. Nath, and C. B. Eom, *Appl. Phys. Lett.* **76**, 2421 (2000).
- <sup>12</sup>J. Dho, Y. N. Kim, Y. S. Hwang, J. C. Kim, and N. H. Hur, *Appl. Phys. Lett.* **82**, 1434 (2003).
- <sup>13</sup>H. Boschker, M. Mathews, E. P. Houwman, H. Nishikawa, A. Vailionis, G. Koster, G. Rijnders, and D. H. A. Blank, *Phys. Rev. B* **79**, 214425 (2009).
- <sup>14</sup>A. Vigliante, U. Gebhardt, A. Rühm, P. Wochner, F. S. Razavi, and H.-U. Habermeier, *Europhys. Lett.* **54**, 619 (2001).
- <sup>15</sup>U. Gebhardt, N. V. Kasper, A. Vigliante, P. Wochner, H. Dosch, F. S. Razavi, and H.-U. Habermeier, *Phys. Rev. Lett.* **98**, 096101 (2007).
- <sup>16</sup>P. G. Radaelli, G. Iannone, M. Marezio, H. Y. Hwang, S.-W. Cheong, J. D. Jorgensen, and D. N. Argyriou, *Phys. Rev. B* **56**, 8265 (1997); A. Senyshyn, L. Vasylechko, M. Knapp, U. Bismayer, M. Berkowski, and A. Matkovskii, *J. Alloys Compd.* **382**, 84 (2004).
- <sup>17</sup>A. Vailionis, W. Siemons, and G. Koster, *Appl. Phys. Lett.* **91**, 071907 (2007).
- <sup>18</sup>A. M. Glazer, *Acta Crystallogr., Sect. A: Found. Crystallogr.* **31**, 756 (1975).